PROCEEDINGS OF SCIENCE

Practical and Accurate Calculations of Radio Emission from Extensive Air Showers

Austin Cummings,[a,*] **Washington Carvalho Jr.,**[b] **Andrew Ludwig**[c] **and Andres Romero-Wolf**[c]

[a] *Departments of Physics and Astronomy & Astrophysics, Institute for Gravitation and the Cosmos, Pennsylvania State University, University Park, PA 16802, USA*

[b] *IMAPP, Radboud University, Nijmegen, the Netherlands*

[c] *Jet Propulsion Laboratory, California Institute of Technology Pasadena, CA 91109, USA*

E-mail: alc6658@psu.edu

Many current and future experiments aim to observe the radio emission produced by air showers sourced from cosmic rays and neutrinos. Extensive simulations of these showers are required to optimize future experimental designs and to accurately reconstruct the parameters of detected events. Traditionally, the vector potential from every particle track in the shower is calculated separately for a given antenna position. This vector potential calculation is computationally expensive, and makes simulation of realistic showers (less thinning) inconvenient due to long computation times.

In this work, we present a novel, semi-analytical treatment of this calculation, whereby multiple tracks within a 4-Dimensional spacetime volume can be treated as one, weighted by the other tracks within the volume. Expensive calculations previously performed on a per-track basis need only to be calculated once for each volume, thereby reducing computation time and complexity. These 4-D volumes can be large while satisfying diffraction limits, capturing many tracks at once, with the number of contained tracks increasing with decreasing thinning (more realistic showers). This method has been shown to reproduce the results of full ZHAireS simulations in a fraction of the time while keeping the precision of the microscopic treatment.

We demonstrate the efficacy of this method by showing comparisons to full microscopic simulations for given shower geometries and highlighting the reduction in computational time and complexity. We discuss the use cases for this method and its limitations as well as future applications.

38th International Cosmic Ray Conference (ICRC2023)
26 July - 3 August, 2023
Nagoya, Japan

*Speaker

© Copyright owned by the author(s) under the terms of the Creative Commons Attribution-NonCommercial-NoDerivatives 4.0 International License (CC BY-NC-ND 4.0).

1. Introduction

Observing ultra-high energy cosmic rays (UHECR) and high energy neutrinos provides a unique opportunity to study the most extreme events occurring in the universe. By measuring the emission from secondaries formed by particle cascades following the interaction of primary particles, we can detect UHECR and high energy neutrinos, which serve as a window to these extraordinary phenomena. Extensive Air Showers (EAS), or particle cascades in air, are particularly intriguing due to their spatial development over kilometers, which help to increase the chance of detection for a given event. While various experiments focus on directly detecting secondary particles or optical (fluorescence or Cherenkov) emission produced by EAS sourced from either UHECR or neutrinos, we focus on the measurement of radio emission from such events.

During the development of an EAS, the secondary particles in the cascade produce coherent radio emission through two mechanisms: the geomagnetic and Askaryan effects. As secondaries within the EAS propagate, charged particles (the vast majority being electrons and positrons), experience deflection from each other due to Earth's geomagnetic field. On a macroscopic scale, this can be thought of as constituting a moving electric dipole, which produces coherent radio emission: the geomagnetic effect. The radio emission from an EAS is primarily dominated by geomagnetic emission, which is highly influenced by the local magnetic field and the geometry of the shower. In addition, propagating secondaries interact with the atmosphere, undergoing Compton, Moller, and Bhabha scattering and positron annihilation. These interactions lead to an overall excess of negative charge, which, on a macroscopic scale, can be thought of as a single charge moving at relativistic speeds, thereby producing coherent radio emission: the Askaryan effect.

The observation of radio emission from EAS induced by cosmic rays has been achieved by numerous experiments across diverse environments, and the measurement and reconstruction techniques of the observed emission are relatively well understood. In recent years, there has been a growing interest in measuring the radio emission from upward-going EAS resulting from ν_τ interactions within the Earth. Notably, the ANITA experiment has reported several events exhibiting this type of phenomenology, including two steeply upward-going events observed by ANITA-I and ANITA-III, as well as four near-horizon events observed by ANITA-IV [1–3] . Understanding the characteristics of these events is a key objective of the PUEO experiment, aiming to investigate and gain deeper insights into their properties [4].

Simulation plays a crucial role in the design of current and future radio experiments for UHECR and neutrino observation by accurately modeling radio emission from EAS, encompassing both geomagnetic and Askaryan production mechanisms. The microscopic approach, one method of simulation, involves calculating and summing the vector potential produced by secondaries on a track-by-track basis (typically generated via an EAS simulation code like Aires [5] or CORSIKA [6]) using equation 1, without presupposing any emission mechanism:

$$\mathbf{A}(\mathbf{x},t) = \frac{\mu_0 q}{4\pi|\vec{R}|}\mathbf{v}_\perp \frac{1}{\left|1 - n_{\text{emit}}\vec{\beta}\cdot\vec{R}\right|}\Pi\left(t', t'_1, t'_2\right) \tag{1}$$

$$t'_{1,2} = \frac{n_{\text{eff}}|\vec{R}|}{c} + t_{1,2} - (n_{\text{emit}}\vec{\beta}\cdot\vec{R})(t_{1,2} - t_0)$$

$$n_{\text{eff}} = 1 + \frac{1}{|\vec{R}|}\int_0^R (1 - n(h))\, dl$$

Where $\vec{R}$ is the line of sight from the center point of the emitting track to the observer, $\mathbf{v}_\perp$ is the projection of the particle velocity onto the plane perpendicular to the line of sight vector, n_{emit} is the index of refraction at the height of the emitter, n_{eff} is the effective index of refraction integrated along the line of sight, t_1, t_0, and t_2 are the start time, midpoint, and end time of the track, and Π is a boxcar function that is equal to 1 between the observer start time, t'_1, and end time, t'_2, of the track, and 0 elsewhere.

While successful in modeling the radio emission from an EAS, the microscopic approach encounters a primary drawback as it becomes increasingly computationally expensive and time-consuming when higher shower resolution is desired. The future radio detection of UHECR and high energy neutrinos envisions extremely large antenna arrays and long-duration flights, necessitating extensive simulations of high-fidelity EAS for downward-going cosmic rays, upward-going neutrino-sourced secondaries, and cosmic rays originating above the horizon and skimming the atmosphere.

Prior macroscopic modeling endeavors successfully parameterize downward-going cosmic ray-induced EAS but fail to function in the geometries required for upward-going neutrino-sourced showers and cosmic rays from above the horizon [7]. An alternative approach, known as radiomorphing, utilizes emission data from a reference shower to model the emission from any arbitrary shower and detector layout. This method scales electric fields and time traces sensibly, treating the emitter as a point source at the shower maximum X_{max} [8]. While the radiomorphing approach closely reproduces the results of the microscopic approach for downward-going cosmic rays at frequencies below 300 MHz, discrepancies arise at higher frequencies, likely due to the limitations of the point-source approximation. Furthermore, the scaling techniques presented by the radiomorphing approach are not valid for upward-going or above-the-horizon EAS geometries. Therefore, a method is needed that can emulate the efficiency of other macroscopic approaches while maintaining the accuracy achieved by the microscopic approach.

2. Approach

The single track formalism calculation of the vector potential detailed in equation 1 can be generalized to a summation of currents in 4-dimensional spacetime by replacing the following quantities with effective values:

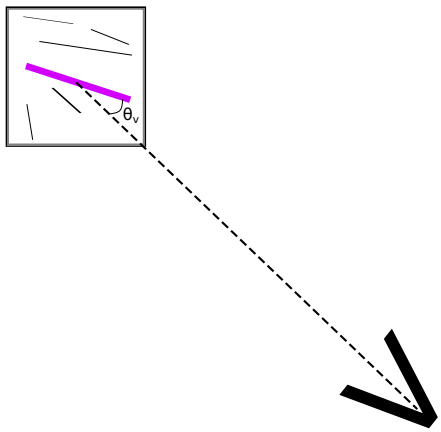

Figure 1: Simplified 2-D diagram of the practical and accurate calculation of radio emission concept. The black square represents a 4-Dimensional cell in space-time within the EAS, while the thin black lines within the cell represent the individual currents from secondary tracks, which added together form the effective current, shown by the thick purple line. The radiation at the detector is calculated using this effective current and the view angle, θ_v

$$\begin{aligned} &\bullet \quad q\mathbf{v} \rightarrow (Q\mathbf{v})_{\text{eff}} = \frac{\sum_j w_j q_j \mathbf{v}_j (t_2 - t_1)_j}{(t_{2,\text{eff}} - t_{1,\text{eff}})} \\ &\bullet \quad \mathbf{X} \rightarrow \mathbf{X}_{\text{eff}} = \frac{\sum_j w_j \mathbf{X}_j}{\sum_j w_j}; \qquad t_{1,2}, \vec{\beta}, \vec{p} \in \mathbf{X} \end{aligned} \tag{2}$$

where w_j corresponds to the weight of a single track (via thinning procedures of the EAS simulation code) and $\vec{p}$ represents the centerpoint coordinates of a single track, which influences the calculations of $\vec{R}$, n_{emit}, and n_{eff} listed in equation 1.

This calculation amounts to a macroscopic treatment of the shower, in that many tracks are effectively averaged over, but microscopic precision is retained by treating the summed currents via equation 1. In the practical and accurate approach described here, we define 4-Dimensional cells in space-time within which particle tracks can be effectively summed. By doing so, computationally exhaustive calculations that typically need to be performed for each individual track (integration for n_{eff}, vector potential summing at observer, etc.), should theoretically only need to be performed once per cell, reducing complexity. The computation time of this approach should decrease with respect to the fully microscopic approach by a factor corresponding to the average number of particle tracks contained within a given 4-D cell. A simplified diagram of the practical and accurate radio calculation concept is shown in Figure 1.

2.1 Cell Size Optimization

The efficiency of the practical and accurate approach is limited by the maximum volume of the 4-D cells, which in turn restricts the number of tracks that can be contained within a single cell.

To disregard higher-order diffraction terms in the emission calculations, the microscopic approach requires that individual track lengths be smaller than the Fraunhofer limit:

$$L < L_F = \frac{1}{\sin\theta}\sqrt{\frac{\lambda|\vec{R}|}{2\pi}} \tag{3}$$

Here, L represents the track length, λ denotes the wavelength of radiation, and θ signifies the angle between the track's center and the observer. Tracks with lengths L exceeding the Fraunhofer limit encounter errors caused by higher-order phase terms approaching $\pm\pi$. In the microscopic approach, tracks with $L > L_F$ are divided into smaller tracks that adhere to Equation 3. A similar principle can be applied to the practical and accurate method, involving 4-D cells with side lengths that obey the Fraunhofer limit. These dimensions define the maximum size of a cell to maintain accuracy and are chosen to be sufficiently small, enabling the averaging of many contributions to the vector potential over the cell.

We use a non-uniform cell size throughout the EAS to account for the Fraunhofer dependence on distance from the observer. In this approach, we begin with large cells of side length $(L, L/c)$ that encompass the entire shower. A minimum cell side length, equal to AL_F, is defined, representing the maximum length that satisfies the Fraunhofer approximation scaled by a factor A. The angular factor θ in Equation 3 is pre-set to 60°, as currents with angles greater than this contribute negligibly to the vector potential. For any given 4-D cell, if the side length is smaller than the locally calculated AL_F, all side lengths of the cell are halved, resulting in eight new subvolumes. Subvolumes that do not contain tracks are disregarded in the final calculation. This strategy is iteratively applied until all cells have side lengths that meet the condition $L < AL_F$. Figure 2 provides a 2-D diagram illustrating this binning, where the left panel depicts the initialization of the binning, and the right panel represents the optimized binning scheme.

3. Comparisons

To demonstrate the potential of the practical and and accurate approach described here, we calculate the radio emission of an example air shower using the methods shown above, where Aires [5] is used to provide the tracks of secondary particles, and then compare to the results of the full microscopic approach using the ZHAireS extension [9]. We consider an EAS initiated by a 1 EeV primary proton with a zenith angle $\theta = 80°$ and a particle thinning level of 10^{-4}, with a single antenna located at P = [500 m, 0 m, 0 m]. To be consistent between the two methodologies, we use the same particle tracks for each calculation. Figure 3 shows the comparison between the two methods in the time and frequency domain for three different cell sizes based on the scaling of the Fraunhofer limit described above.

Figure 3 shows that the practical and accurate approach closely reproduces the characteristics of the radio emission generated using the full microscopic approach via ZHAireS simulations. Calculations using smaller cell sizes in particular emulate the frequency spectra out to 1 GHz, while for larger cell sizes (up to L_F), only behavior below tens of MHz is captured well. For more realistic showers with less thinning (more tracks contained per 4-D cell), the high frequency behavior is

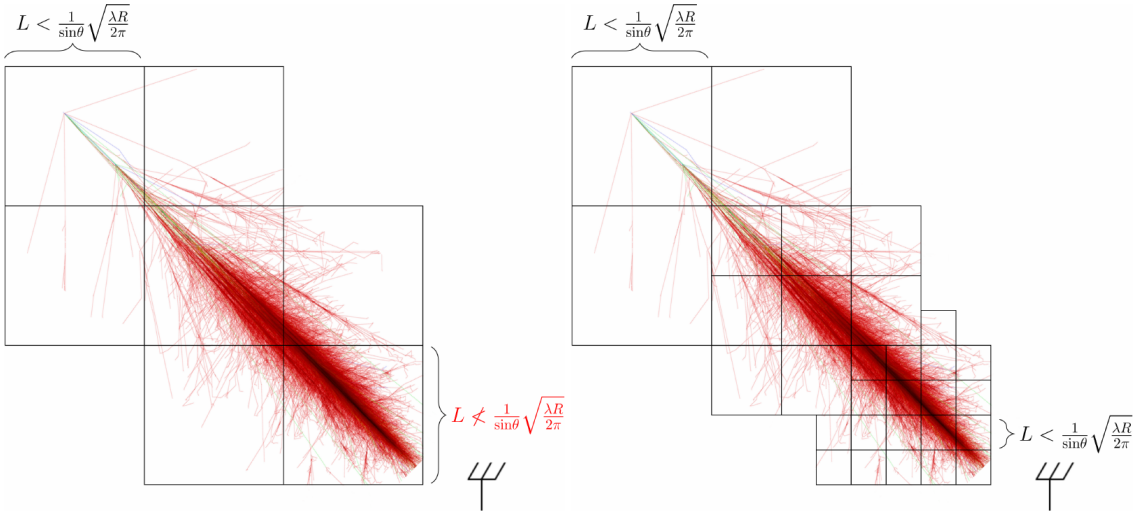

Figure 2: Diagram of the 4-Dimensional binning method of an EAS. Cells are initialized to be very large to capture as many particle tracks as possible. If the side length of a cell does not meet a minimum size set by the method (typically some multiple of the Fraunhofer approximation, shown in equation 3), it is subdivided into eight equal volumes, such that binning of the shower tracks takes place over unequal sized 4-D volumes. Subvolumes that do not contain tracks are ignored. Shower image taken from CORSIKA simulation [6].

worsened across all cell sizes, implying a systematic discrepancy when summing many tracks within a cell. This discrepancy will be investigated and quantified in future work. The average number of tracks contained in a 4-D cell with side length L_F is on the order of ~ 10 in the case shown above, and will grow inversely with decreased thinning. Thus, we expect an orders of magnitude decrease in computation time using the practical and accurate approach with respect to the full microscopic simulation.

4. Summary and Outlook

The practical and accurate approach to the calculation of radio emission using 4-Dimensional binning demonstrates strong potential for use in future simulations of EAS. It has been shown to largely reproduce the vector potential and electric field generated by the microscopic approach via ZHAireS simulations, while performing roughly 10 times fewer overall calculations. The performance gains from the practical and accurate approach will grow with increasingly realistic showers, offering an orders of magnitude reduction in computation time with respect to the microscopic approach. Systematic differences between the two methods exist at high frequencies, and will be investigated in future work.

In addition to being used for production scale simulations for designing and evaluating current and future radio detectors, there are several specific use cases for the practical and accurate approach that we envision proving helpful in the field of UHECR and neutrino research: i) Previous simulations of the radio emission from neutrino-sourced upwards going EAS have given rise to anomalous behavior in rarified atmosphere that needs to be verified. The macroscopic approach

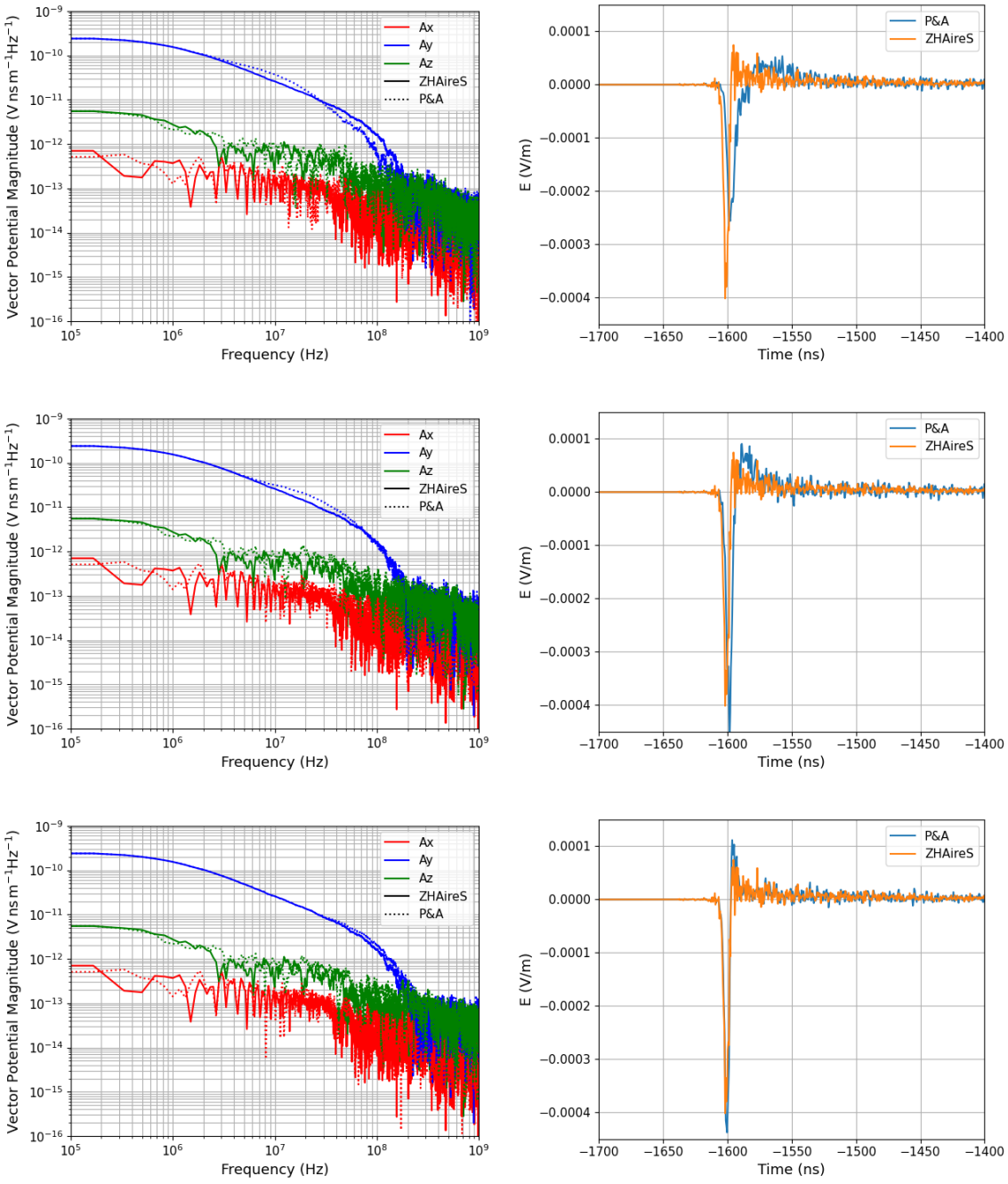

Figure 3: Comparison of radio emission produced by a downward going cosmic ray induced EAS, as calculated with ZHAireS and the practical and accurate approach described in this work. The left columns show the frequency spectra of the vector potential magnitude for the different polarization states while the right columns show the time domain electric field. The rows represent different scalings of the Fraunhofer limit to determine the side length of a 4-D cell, with the top, middle, and bottom rows corresponding to L_F, $0.5L_F$, and $0.1L_F$. All cell sizes assume a maximum frequency of 1 GHz.

allows for spherical propagation of radiation not present in microscopic simulations which may solve the disparity. ii) The simulation of radio emission from near-horizon cosmic ray sourced EAS is typically difficult to model in microscopic simulations due to the nontrivial modeling of the atmosphere. Using the practical and accurate approach, the only thing that should be modified to model these EAS is the effective index of refraction n_{eff} calculation. Such simulations will help evaluate background event rate estimations for high altitude radio experiments. iii) Studying the impact of atmospheric variations on signal properties using the microscopic approach can be complicated and computationally exhaustive. The practical and accurate approach should help alleviate these calculations and help to bound future observations of the emission. iv) Radio emission from in-ice particle cascades has been fairly successfully parameterized to provide fast and accurate results for large scale simulation studies. However, this approach may be extendable to the medium and can help to resolve near-field effects and the influence of nontrivial ice density gradients.

The practical and accurate approach to calculating radio emission of EAS presented in this work represents a useful and complimentary approach to calculations via the microscopic approach and other available macroscopic methods. Future work will be performed to further refine the methods described in this work and to better quantify the expected performance gains.

References

[1] (ANITA) collaboration, *Characteristics of Four Upward-Pointing Cosmic-Ray-like Events Observed with ANITA*, *Phys. Rev. Lett.* **117** (2016) 071101.

[2] (ANITA) collaboration, *Observation of an Unusual Upward-going Cosmic-ray-like Event in the Third Flight of ANITA*, *Phys. Rev. Lett.* **121** (2018) 161102 [1803.05088].

[3] ANITA collaboration, *Unusual Near-Horizon Cosmic-Ray-like Events Observed by ANITA-IV*, *Phys. Rev. Lett.* **126** (2021) 071103 [2008.05690].

[4] The PUEO Collaboration, *The payload for ultrahigh energy observations (PUEO): a white paper*, *Journal of Instrumentation* **16** (2021) P08035.

[5] S J Sciutto, *Aires a system for air shower simulations. user's guide and reference manual*, .

[6] D. Heck, J. Knapp, J.N. Capdevielle, G. Schatz and T. Thouw, *CORSIKA: a Monte Carlo code to simulate extensive air showers.* (1998).

[7] O. Scholten, T.N.G. Trinh, K.D. de Vries and B.M. Hare, *Analytic calculation of radio emission from parametrized extensive air showers: A tool to extract shower parameters*, *Phys. Rev. D* **97** (2018) 023005 [1711.10164].

[8] A. Zilles, O. Martineau-Huynh, K. Kotera, M. Tueros, K. de Vries, W. Carvalho et al., *Radio morphing: towards a fast computation of the radio signal from air showers*, *Astroparticle Physics* **114** (2020) 10.

[9] J. Alvarez-Muñiz, W.R. Carvalho and E. Zas, *Monte carlo simulations of radio pulses in atmospheric showers using ZHAireS*, *Astroparticle Physics* **35** (2012) 325.